TITLE:

Deep levels induced by reactive ion etching in n- and p-type 4H-SiC

AUTHOR(S):

Kawahara, Koutarou; Krieger, Michael; Suda, Jun; Kimoto, Tsunenobu

CITATION:

Kawahara, Koutarou ...[et al]. Deep levels induced by reactive ion etching in n- and p-type 4H-SiC. JOURNAL OF APPLIED PHYSICS 2010, 108(2): 023706.

ISSUE DATE:

2010-07

URL:

http://hdl.handle.net/2433/147211

RIGHT:

Copyright 2010 American Institute of Physics. This article may be downloaded for personal use only. Any other use requires prior permission of the author and the American Institute of Physics. The following article appeared in JOURNAL OF APPLIED PHYSICS108, 023706 (2010) and may be found at

京都大学学術情報リポジトリ
KURENAI
Kyoto University Research Information Repository

京都大学 KYOTO UNIVERSITY
A Self-archived copy in
Kyoto University Research Information Repository
https://repository.kulib.kyoto-u.ac.jp
京都大学学術情報リポジトリ KURENAI 紅 Kyoto University Research Information Repository

JOURNAL OF APPLIED PHYSICS **108**, 023706 (2010)

Deep levels induced by reactive ion etching in n- and p-type 4H–SiC

Koutarou Kawahara,[1,a)] Michael Krieger,[2] Jun Suda,[1] and Tsunenobu Kimoto[1]
[1]*Department of Electronic Science and Engineering, Kyoto University, Katsura, Nishikyo, Kyoto 615-8510, Japan*
[2]*Lehrstuhl für Angewandte Physik, Universität Erlangen- Nürnberg, Staudtstr. 7/A3, D-91058 Erlangen, Germany*

(Received 1 April 2010; accepted 6 June 2010; published online 27 July 2010)

In this study, the authors investigate deep levels, which are induced by reactive ion etching (RIE) of n-type/p-type 4H–SiC, by deep level transient spectroscopy (DLTS). The capacitance of a Schottky contact fabricated on as-etched p-type SiC is abnormally small due to compensation or deactivation of acceptors extending to a depth of ~14 μm, which is nearly equal to the epilayer thickness. The value of the capacitance can recover to that of a Schottky contact on as-grown samples after annealing at 1000 °C. However, various kinds of defects, IN2 ($E_C-0.30$ eV), EN ($E_C-1.6$ eV), IP1 ($E_V+0.30$ eV), IP2 ($E_V+0.39$ eV), IP4 (HK0: $E_V+0.72$ eV), IP5 ($E_V+0.85$ eV), IP7 ($E_V+1.3$ eV), and EP ($E_V+1.4$ eV), remain at a high concentration (average of total defect concentration in the region ranging from 0.3 μm to 1.0 μm: $\sim 5\times10^{14}$ cm^{-3}) even after annealing at 1000 °C. The concentration of all these defects generated by RIE, except for the IP4 (HK0) center, remarkably decreases by thermal oxidation. In addition, the HK0 center can also be reduced significantly by a subsequent annealing at 1400 °C in Ar. © *2010 American Institute of Physics*. [doi:10.1063/1.3460636]

I. INTRODUCTION

SiC has unique and fascinating features, like, e.g., large breakdown electric field (about 3 MV/cm), high thermal stability, which are advantageous for fabricating high-power, high-temperature, and high-frequency devices. In general, deep levels, which have several harmful effects on the device performance such as reduction in conductivity and limitation of minority carrier lifetimes, are generated in SiC either directly during the crystal growth or afterwards by ion implantation. So far, a great number of investigations have been published on deep levels in as-grown and irradiated 4H–SiC.[1–10] In addition, several groups have investigated deep levels that are introduced by device processing like ion implantation.[1,11–16] However, detailed study on deep levels generated by the etching process has not been reported. The reactive ion etching (RIE) is an essential process for fabrication of SiC devices such as mesa diodes and trench metal-oxide-semiconductor field-effect transistors, which require the etching of high aspect-ratio and selectivity. However, lattice damage by ion bombardment is a negative effect of RIE. For example, reduction in barrier height and degradation in forward characteristics by RIE damage in 4H–SiC Schottky barrier diodes have been reported.[17]

II. EXPERIMENTS

The starting materials were N-doped n-type or Al-doped p-type 4H–SiC (0001) epilayers with a doping concentration of $(7-8)\times10^{15}$ cm^{-3}. For the *C-V* and deep level transient spectroscopy (DLTS) measurements, Ni and Ti were employed as Schottky contacts on n- and p-type samples, respectively. The typical diameter of Schottky contacts was 1 mm. A Ti/Al/Ni (20 nm/100 nm/80 nm) layer annealed at 1000 °C for 2 min was employed as backside Ohmic contacts for p-type materials. Deep levels located in the upper half of the band gap can be monitored by using n-type epilayers, and deep levels in the lower half of the band gap by using p-type materials. A period width of 0.205 s was employed for all DLTS measurements performed in this study. A typical reverse bias is −1 V (for n-type) or 1 V (for p-type) and pulse voltage is 0 V, under which condition all DLTS spectra shown in this paper were obtained (the observed depth was around 0.2 μm from the surface). The reverse and pulse voltages were accordingly changed in order to obtain depth profile of defect concentration. After the measurements taken on as-grown samples, RIE was performed for 7 min under a standard condition (CF_4: 5 SCCM, O_2: 10 SCCM, rf power: 150 W, pressure: 20 Pa), by which a layer of about 0.9 μm was etched off from the surface. After the etching, new Schottky contacts were prepared and *C-V* and DLTS measurements were repeated. An overview of experimental procedure is shown in Fig. 1.

III. RESULTS

A. *C-V* characteristics

Figures 2 and 3 show the $1/C^2$-V plots obtained from n- and p-type 4H–SiC, respectively, for an as-grown epilayer (closed circles), sample after RIE (triangles), and sample after RIE plus annealing at 1000 °C for 30 min in Ar ambient (squares). The solid (as-grown), broken (RIE), and dotted (RIE+annealing) lines show the corresponding fitting. The fitting procedure was conducted by using the doping concentration (N_d or N_a) and the thickness of the compensated region d_C as parameters. In n-type samples, the doping concentration increased after RIE, which may indicate the

a)Electronic mail: kawahara@semicon.kuee.kyoto-u.ac.jp.

 © 2010 American Institute of Physics

Downloaded 19 Jun 2011 to 130.54.110.71. Redistribution subject to AIP license or copyright; see http://jap.aip.org/about/rights_and_permissions

京都大学 KYOTO UNIVERSITY
A Self-archived copy in
Kyoto University Research Information Repository
https://repository.kulib.kyoto-u.ac.jp
京都大学学術情報リポジトリ KURENAI 紅 Kyoto University Research Information Repository

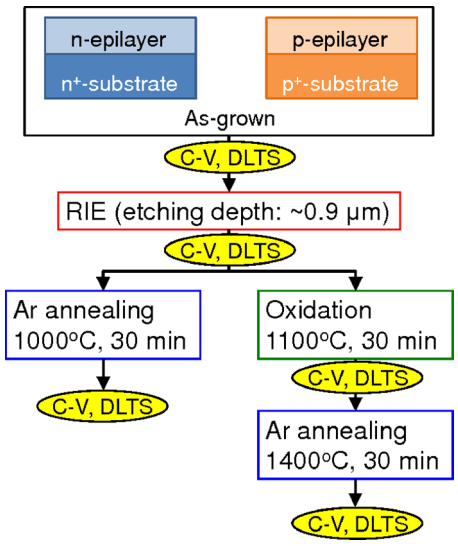

FIG. 1. (Color online) Experimental procedure to investigate RIE damage and the reduction.

generation of unknown shallow donors. On the other hand, the capacitance of the p-type samples was extremely decreased after the RIE process. The capacitance value was about 5 pF (compared to about 120 pF at 0 V prior to RIE) and stayed almost independent of the bias. The small and constant capacitance of RIE-etched p-type SiC indicates the existence of a compensated or deactivated region. In view of 5 pF with a contact size $\Phi=1$ mm, the thickness of the compensated region is estimated to be about 14 μm, which is surprisingly almost equal to the complete epilayer thickness. Due to the fact that the as-etched p-type samples could not be characterized by DLTS because of the severe compensation (or deactivation of acceptors), a subsequent annealing was performed at 1000 °C for 30 min. After this annealing step, the *C-V* characteristics were recovered to those of as-grown samples. The authors also found that the capacitances could be recovered by the 1000 °C-annealing for only 2 min.

It is unlikely that the 14 μm-thick depletion region is attributed to lattice damage introduced by ion bombardment during RIE process because the acceleration energy of impinging ions is only several hundred electron volt at the highest. Note that an implanted fluorine with 500 eV reaches below the depth of 4 nm, which is simulated by a SRIM (Ref. 18) code. Therefore, the authors speculate that the thick depletion-region may be caused by permeation of some atoms during RIE process, which was observed in Si.[19] In Si, shallow acceptors are passivated by hydrogen permeation, which recovers to an original state by annealing at 200 °C.[20] Depth profiles of impurities obtained by secondary ion mass spectrometry (SIMS) for RIE-etched p-type 4H–SiC are shown in Fig. 4. The closed circles, closed triangles, and

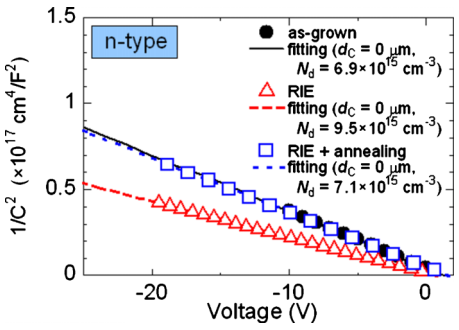

FIG. 2. (Color online) $1/C^2$-V plots obtained from as-grown (closed circles) n-type 4H–SiC, after RIE (triangles), and after RIE plus annealing at 1000 °C (squares). The solid, broken, and dotted lines are the fitting lines to the corresponding experimental data (N_d: donor concentration, d_C: thickness of the compensated region).

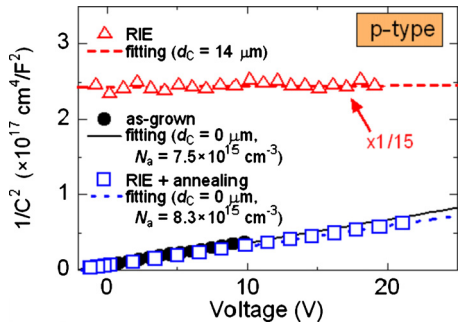

FIG. 3. (Color online) $1/C^2$-V plots obtained from as-grown (closed circles) p-type 4H–SiC, after RIE (triangles), and after RIE plus annealing at 1000 °C (squares). The solid, broken, and dotted lines are the fitting lines to the corresponding experimental data (N_a: acceptor concentration, d_C: thickness of the compensated region).

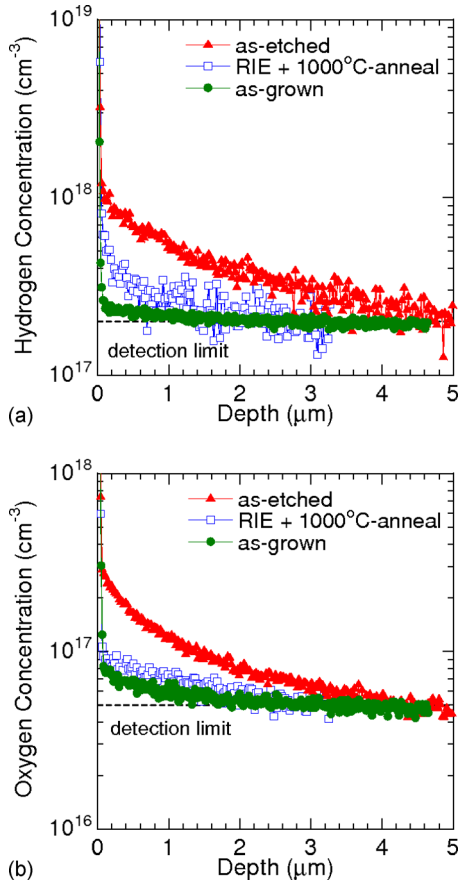

FIG. 4. (Color online) (a) Hydrogen and (b) oxygen depth profiles obtained by SIMS for as-grown (closed circles) p-type 4H–SiC, after RIE (closed triangles), and after RIE plus annealing at 1000 °C (squares).

Downloaded 19 Jun 2011 to 130.54.110.71. Redistribution subject to AIP license or copyright; see http://jap.aip.org/about/rights_and_permissions

京都大学 KYOTO UNIVERSITY
A Self-archived copy in
Kyoto University Research Information Repository
https://repository.kulib.kyoto-u.ac.jp
京都大学学術情報リポジトリ KURENAI 紅 Kyoto University Research Information Repository

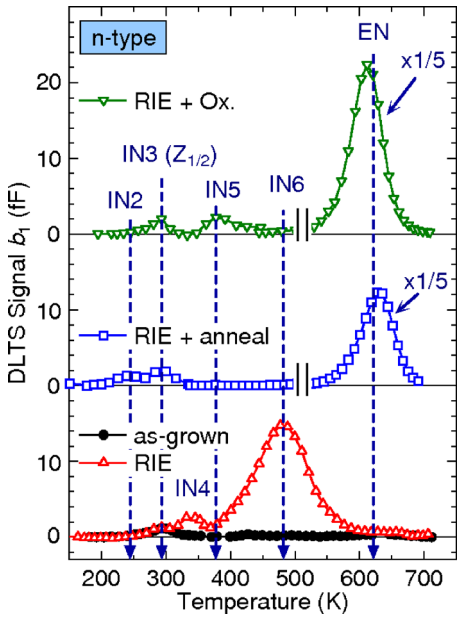

FIG. 5. (Color online) DLTS spectra obtained from as-grown (closed circles) and as-etched (triangles) n-type 4H–SiC. The spectra from the samples annealed at 1000 °C in Ar ambient after RIE (squares) and the samples oxidized at 1100 °C after RIE (inverse triangles) are also shown.

squares correspond to as-grown p-type 4H–SiC, after RIE, and after RIE plus annealing at 1000 °C, respectively. Hydrogen [Fig. 4(a)] and oxygen [Fig. 4(b)] atoms clearly permeated the samples after RIE, while fluorine atoms (not shown) did not. Hydrogen atoms may come from H_2O remaining in the RIE chamber, and oxygen atoms may come from O_2 gas. The fluorine concentration in the RIE-etched sample (below 3×10^{15} cm^{-3}, which is nearly equal to the detection limit) was clearly below the doping concentration (about 8×10^{15} cm^{-3}). The result indicates that fluorine atoms do not cause the formation of the depletion region. Although it is difficult to conclude, the origin of the thick depletion region is more likely to be the permeating oxygen than hydrogen because a high concentration of hydrogen atoms (over 2×10^{17} cm^{-3}) still remained near the surface after annealing at 1000 °C while the oxygen concentration decreased to the value of the as-grown sample. Some oxygen-related defects act as shallow donors in SiC,[21] which agrees with the result of this study (Fig. 2) although annealing behavior of defects obtained in this study differs from that reported in Ref. 21.

B. DLTS spectra of n-type materials

Figure 5 shows the DLTS spectra obtained from as-grown (closed circles) and as-etched (triangles) n-type 4H–SiC. The figure also shows the DLTS spectra from the samples annealed at 1000 °C in Ar ambient after RIE (squares) and the samples oxidized at 1100 °C after RIE (inverse triangles). In DLTS spectra for n-type as-grown samples, no change was observed after annealing at 1000 °C (not shown). All the DLTS spectra shown in this paper monitor deep levels located at a depth of about 0.2 μm from the surface. After the RIE process, large DLTS peaks, IN4 ($E_C-0.65$ eV) and IN6 ($E_C-1.0$ eV), emerged while IN3 [$Z_{1/2}$ (Ref. 1): $E_C-0.63$ eV] was also observed in an as-grown sample. Deep levels named "INn" ($n=1,2,3\ldots$) are the same defect centers as those detected in ion (Al^+, N^+, P^+, or Ne^+)-implanted n-type 4H–SiC.[14] The IN4 and IN6 centers exist only near the surface shallower than the depth of about 0.5 μm. After the intentional annealing at 1000 °C for 30 min, the IN4 and IN6 centers disappeared. These thermally unstable centers, IN4 and IN6, may be assigned to the ET2 [may be EH_3 (Ref. 6)] and ET3 [may be RD_3 (Ref. 1)] centers, respectively, which are generated by electron irradiation at low energy (116 keV) and drastically reduced by annealing at 950 °C for 30 min in Ar.[22] The IN4 and IN6 centers also correspond to the HR_2 (Ref. 23) and EH_5 (Ref. 6) centers, respectively. The HR_2 center was detected in H^+-implanted 4H–SiC and disappeared after annealing at 800 °C for 20 min in N_2,[23] while the EH_5 center was observed in electron-irradiated (2.5 MeV,[6] 15 MeV[23]) and H^+-implanted[23] 4H–SiC, which disappeared after annealing at 600 °C for 20 min in N_2.[23] On the other hand, after the 1000 °C-annealing, the EN center ($E_C-1.6$ eV) was observed as a dominant defect generated at high concentration ($>1\times10^{15}$ cm^{-3}), as shown by squares in Fig. 5. The IN2 ($E_C-0.30$ eV) center appeared after the annealing, which may consist with the ID_8 center[1,11] detected in (Ti^+, V^+, or Al^+)-implanted n-type 4H–SiC after annealing at 1700 °C for 30 min. Therefore, the annealing at 1000 °C is not sufficient for annihilation of the point defects generated by RIE. Since thermal oxidation was revealed to be effective for the reduction in deep levels in as-grown samples,[24] the authors tried to reduce deep levels detected in etched samples by dry oxidation at 1100 °C for 30 min in 100% O_2 ambient (the thickness of the formed SiO_2 layer was about 5 nm). Post-oxidation annealing was not performed. The result is shown by the inverse triangles in Fig. 5. After oxidation, the IN2 detected in the annealed sample is significantly decreased. A new defect generated by the oxidation is IN5 ($E_C-0.73$ eV), which exists only near the surface (<0.4 μm). The IN5 center may be assigned to the EH_4 center observed in electron-irradiated (2.5 MeV,[6] 15 MeV[23]) and H^+-implanted[23] 4H–SiC. The parameters of the deep levels detected in RIE-etched n-type 4H–SiC are summarized in Table I. The corresponding centers were determined from the energy levels and the thermal stability.

Figure 6 shows the depth profile of the EN defect in the RIE-etched n-type 4H–SiC after annealing at 1000 °C (squares) or after oxidization (inverse triangles). The dominant deep level detected after RIE plus 1000 °C-annealing, EN center, exists at a high concentration near the surface ($\sim1\times10^{15}$ cm^{-3} at 0.1 μm from the surface), while at a relatively low concentration ($\sim4\times10^{13}$ cm^{-3}) in deeper region (>0.2 μm). The EN center is a stable deep level, which cannot be reduced by thermal oxidation near the surface.

C. DLTS spectra of p-type materials

Figure 7 shows the DLTS spectra obtained from as-grown (closed circles) and RIE-etched p-type 4H–SiC with annealing at 1000 °C (squares). The figure also shows the

Downloaded 19 Jun 2011 to 130.54.110.71. Redistribution subject to AIP license or copyright; see http://jap.aip.org/about/rights_and_permissions

京都大学 KYOTO UNIVERSITY
A Self-archived copy in
Kyoto University Research Information Repository
https://repository.kulib.kyoto-u.ac.jp
京都大学学術情報リポジトリ KURENAI 紅 Kyoto University Research Information Repository

TABLE I. Energy positions and capture cross-sections of deep levels observed in RIE-etched n-type 4H–SiC (σ: the capture cross-section, N_T: the average of trap concentration from the depth of 0.3 to 1.0 μm in SiC after RIE, after RIE+annealing at 1000 °C, and after RIE+oxidation at 1100 °C).

Label	E_C-E_T (eV)	σ (cm^2)	N_T (cm^{-3}) RIE	RIE+anneal	RIE+ox.	Corresponding center
IN2	0.30	10^{-18}	Not observed	1×10^{13}	Not observed	ID_8 [a,b]
IN3	0.63	10^{-14}	3×10^{13}	3×10^{13}	1×10^{13}	$Z_{1/2}$ [a]
IN4	0.65	10^{-16}	1×10^{13}	Not observed	Not observed	ET2,[c] EH_3,[d] HR_2 [e]
IN5	0.73	10^{-16}	Not observed	Not observed	4×10^{12}	EH_4 [d]
IN6	1.0	10^{-15}	3×10^{14} [f]	Not observed	Not observed	ET3,[c] RD_3,[a] EH_5 [d]
EN	1.6	10^{-13}	Not observed	2×10^{15} [f]	3×10^{15} [f]	

[a]Reference 1.
[b]Reference 11.
[c]Reference 22.
[d]Reference 6.
[e]Reference 23.
[f]The value obtained at the depth of <0.2 μm. (The level exists only in the shallow region.)

DLTS spectrum of the oxidized sample after RIE with (rhombuses) or without (inverse triangles) subsequent annealing at 1400 °C for 30 min in Ar ambient. The as-etched sample could not be measured due to the severe compensation (or deactivation) as discussed in Sec. III A. While the DLTS spectrum of an as-grown sample exhibited negligibly small peaks, the etched sample annealed at 1000 °C showed large DLTS peaks assigned to IP1 (E_V+0.30 eV), IP2 [HS1 (Refs. 2 and 4)]: E_V+0.39 eV), IP4 (E_V+0.72 eV), IP5 (E_V+0.85 eV), IP7 (E_V+1.3 eV), and EP (E_V+1.4 eV). Deep levels named "IPm" (m=1,2,3…) are the same defect centers as those detected in ion (Al^+, N^+, P^+, or Ne^+)-implanted p-type 4H–SiC.[14] The IP4, IP5, IP7, and EP (maybe IP8), respectively, correspond to HK0, HK2, HK3, and HK4 detected in RIE-etched p-type 4H–SiC after annealing at 950 °C for 30 min in Ar ambient.[5] The IP1 center may be the same as a defect UK1 from the energy level, which is one of dominant peaks in electron-irradiated p-type 4H–SiC after annealing at 950 °C.[5] Among the observed peaks, the EP center exists at high concentration of over 1 $\times10^{14}$ cm^{-3}. Although the EP center decreases in the oxidized sample (inverse triangles), the IP4 (HK0) center increases by oxidation. In order to reduce the HK0 center, the oxidized sample was annealed at 1400 °C for 30 min in Ar ambient. The result is shown by the rhombuses in Fig. 7. After 1400 °C-annealing, almost all the defects generated by RIE significantly decreased. This result supports that the observed levels, IP1, IP5, IP7, and EP are, respectively, UK1, HK2, HK3, and HK4, which can be reduced by annealing at temperatures above 1350 °C.[5] The parameters of the deep levels detected in RIE-etched p-type 4H–SiC are summarized in Table II.

Figure 8(a) shows the depth profile of the HK0 defect in the RIE-etched p-type 4H–SiC after annealing at 1000 °C (squares). The figure also shows the profile of the HK0 defect in the oxidized sample after RIE with (rhombuses) or without (inverse triangles) subsequent annealing in Ar at 1400 °C. The HK0 center is generated to a deep region over

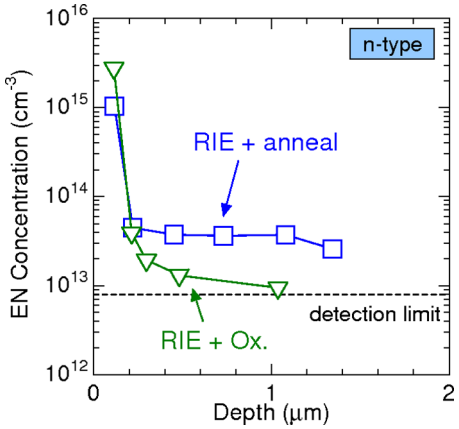

FIG. 6. (Color online) Depth profile of the EN defect in the RIE-etched n-type 4H–SiC after annealing at 1000 °C (squares) or after oxidization at 1100 °C (inverse triangles).

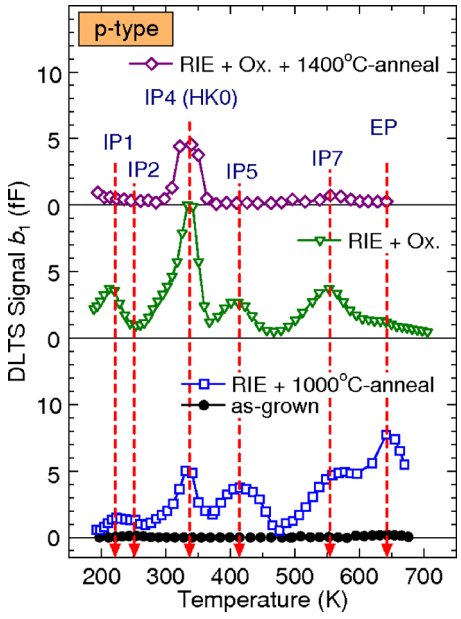

FIG. 7. (Color online) DLTS spectra obtained from as-grown (closed circles) and RIE-etched p-type 4H–SiC with annealing at 1000 °C (squares). The spectra from oxidized samples after RIE with (rhombuses) or without (inverse triangles) subsequent annealing at 1400 °C in Ar ambient are also shown.

Downloaded 19 Jun 2011 to 130.54.110.71. Redistribution subject to AIP license or copyright; see http://jap.aip.org/about/rights_and_permissions

京都大学 KYOTO UNIVERSITY
A Self-archived copy in
Kyoto University Research Information Repository
https://repository.kulib.kyoto-u.ac.jp
京都大学学術情報リポジトリ KURENAI 紅 Kyoto University Research Information Repository

TABLE II. Energy positions and capture cross-sections of deep levels observed in RIE-etched p-type 4H–SiC (σ: the capture cross-section, N_T: the average of trap concentration from the depth of 0.3 to 1.0 μm in SiC after RIE+1000 °C-annealing, after RIE+oxidation at 1100 °C, and RIE+oxidation +1400 °C-annealing).

Label	E_T-E_V (eV)	σ (cm^2)	N_T (cm^{-3}) RIE+1000 °C-anneal	RIE+ox.	RIE+ox.+1400 °C-anneal	Corresponding center
IP1	0.30	10^{-18}	2×10^{13}	5×10^{13}	Not observed	UK1[a]
IP2	0.39	10^{-18}	2×10^{13}	Not observed	Not observed	HS1[b,c]
IP4	0.72	10^{-16}	9×10^{13}	2×10^{14}	8×10^{13}	HK0[a]
IP5	0.85	10^{-16}	4×10^{13}	6×10^{13}	Not observed	HK2[a]
IP7	1.3	10^{-14}	7×10^{13}	4×10^{13}	5×10^{12}	HK3[a]
EP	1.4	10^{-16}	2×10^{14}	2×10^{13}	3×10^{12}	IP8,[d] HK4[a]

[a]Reference 5.
[b]Reference 2.
[c]Reference 4.
[d]Reference 14.

1 μm by RIE (and 1000 °C-annealing), and increased to over 1×10^{14} cm^{-3} after the thermal oxidation. However, the subsequent annealing at 1400 °C for 30 min reduces the HK0 center by a factor of 2 to 3. The HK0 concentration can become lower by extending the annealing time.

Figure 8(b) shows the depth profile of the EP defect in the RIE-etched p-type 4H–SiC after annealing at 1000 °C (squares). The figure also shows the profile of the EP defect in the oxidized sample after RIE with (rhombuses) or without (inverse triangles) subsequent annealing at 1400 °C. The EP concentration in the sample annealed at 1000 °C is high (over 1×10^{14} cm^{-3}) from the near-surface region to a deep region over 1 μm. However, the EP center can be reduced by thermal oxidation as shown by the inverse triangles in Fig. 7, unlike the HK0 center. Additionally, the EP concentration decreases to the detection limit after the subsequent annealing at 1400 °C.

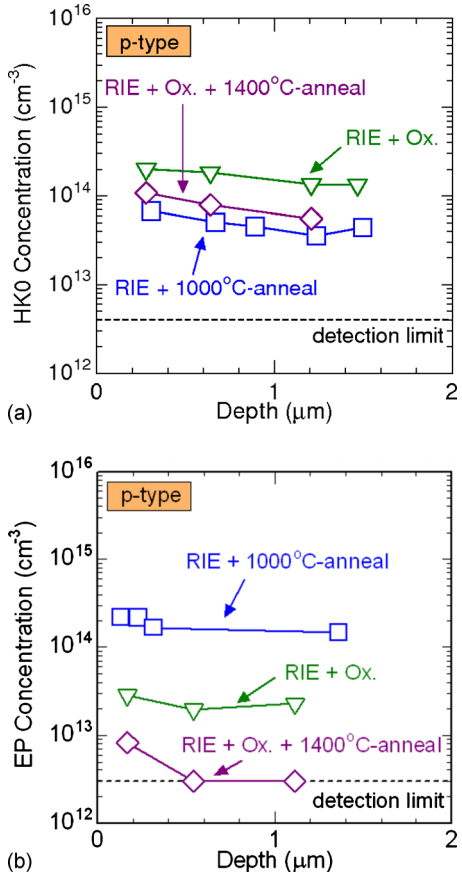

FIG. 8. (Color online) Depth profiles of the (a) IP4 (HK0) and (b) EP defect in the RIE-etched p-type 4H–SiC after annealing at 1000 °C (squares). The profiles of the HK0 defect in the oxidized samples after RIE with (rhombuses) or without (inverse triangles) subsequent annealing at 1400 °C are also shown.

IV. DISCUSSION

As discussed in Sec. III, the dry etching process generates a variety of deep defects in n-type and p-type 4H–SiC. Figure 9 shows the overview of deep levels detected in RIE-

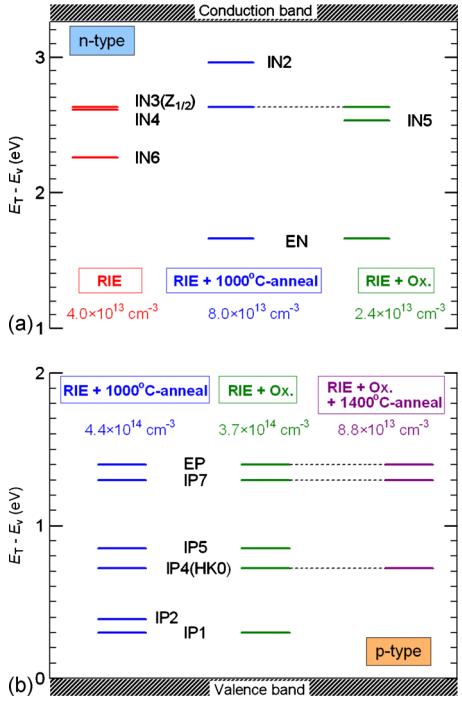

FIG. 9. (Color online) Overview of deep levels detected in RIE-etched (a) n-type and (b) p-type 4H–SiC. The value indicated below each process is the average of the total trap concentration from the depth of 0.3 to 1.0 μm in each sample.

Downloaded 19 Jun 2011 to 130.54.110.71. Redistribution subject to AIP license or copyright; see http://jap.aip.org/about/rights_and_permissions

京都大学 KYOTO UNIVERSITY
A Self-archived copy in
Kyoto University Research Information Repository
https://repository.kulib.kyoto-u.ac.jp
京都大学学術情報リポジトリ KURENAI 紅 Kyoto University Research Information Repository

etched (a) n-type and (b) p-type 4H–SiC. In particular, the capacitance of p-type samples is extremely low after RIE, which indicates that the acceptors are compensated by generated defects or are deactivated. This compensation or deactivation in p-type 4H–SiC must occur during the RIE process while the extent (thickness of the depletion region) depends on the RIE condition. Therefore, when RIE is applied for SiC-device fabrication, subsequent annealing is an essential process. Depth profiles obtained by SIMS for RIE-etched samples indicate that the compensation or deactivation might originate from oxygen permeation by RIE. However, further investigation is required to prove this speculation. In particular, the role of oxygen and oxygen-related defects should be investigated in the future.

Although the low capacitance can be recovered by annealing at 1000 °C, several deep defects remain. Based on DLTS investigations, the energy levels and the corresponding depth profiles of the major deep defects were determined. The INn (n=2,3,4,5,6) and IPm (m=1,2,4,5,7) centers are the same defects as those detected in ion (Al^+, N^+, P^+, or Ne^+)-implanted 4H–SiC, which may originate from intrinsic defects because all these levels were observed in ion-implanted samples irrespective of the implanted species.[14] All of them (except for IN2) and EP (maybe IP8) centers are also observed in electron-irradiated samples (the corresponding centers are shown in Tables I and II), which indicates that these deep levels may originate from intrinsic defect. The IN4 (E_C−0.65 eV), IN6 (E_C−1.0 eV), and EN (E_C −1.6 eV) centers exist only in the near-surface region and may be specific defects generated by RIE. In particular, the EN center shows an extremely high concentration over 1×10^{15} cm^{-3} at the depth of 0.1 μm from the surface. In p-type 4H–SiC, the IP4 (HK0: E_V+0.72 eV) and EP (E_V +1.4 eV) centers, which exhibit rather flat depth profiles and high concentration, are the important defects. The EP center can be reduced by thermal oxidation, while the HK0 center increases. A subsequent annealing step at 1400 °C clearly reduces the HK0 concentration. As a consequence of the results of our study, RIE-etched 4H–SiC should be oxidized and annealed at 1400 °C in order to reduce the major portion of deep levels generated in the band gap of 4H–SiC. Because the EN center remain near the surface region (not shown) even after the oxidation and annealing process, further investigation is necessary for elimination of deep levels generated by RIE. As candidates for the solution, the authors consider removal of the surface by gas etching or optimization of RIE-etching conditions.

V. SUMMARY

In this study, the impact of RIE process on deep levels in n- and p-type 4H–SiC was investigated. In as-etched p-type samples, a thick depletion region was formed, which disappears after annealing at 1000 °C. However, many deep levels remain in the samples even after annealing at 1000 °C. The typical concentration of the deep levels near the surface after RIE plus annealing at 1000 °C is 2×10^{13} cm^{-3} in the upper half of the band gap and 7×10^{13} cm^{-3} in the lower half. Since almost all of these levels are also observed in ion-implanted and electron-irradiated 4H–SiC, these levels may originate from the intrinsic defects. The levels generated by RIE are significantly reduced by thermal oxidation at 1100 °C and subsequent annealing at 1400 °C except for the EN center (E_C−1.6 eV), which shows $\sim1\times10^{15}$ cm^{-3} near the surface region.

ACKNOWLEDGMENTS

This work was supported in part by a Grant-in-Aid for Scientific Research (Grant No. 21226008) from the Japan Society for the Promotion of Science and by the Global COE Program (C09) from the Ministry of Education, Culture, Sports, Science, and Technology, Japan.

[1] T. Dalibor, G. Pensl, H. Matsunami, T. Kimoto, W. J. Choyke, A. Schöner, and N. Nordell, Physica Status Solidi A **162**, 199 (1997).
[2] L. Storasta, J. P. Bergman, E. Janzén, A. Henry, and J. Lu, J. Appl. Phys. **96**, 4909 (2004).
[3] K. Danno and T. Kimoto, J. Appl. Phys. **100**, 113728 (2006).
[4] L. Storasta, F. H. C. Carlsson, S. G. Sridhara, J. P. Bergman, A. Henry, T. Egilsson, A. Hallén, and E. Janzén, Appl. Phys. Lett. **78**, 46 (2001).
[5] K. Danno and T. Kimoto, J. Appl. Phys. **101**, 103704 (2007).
[6] C. Hemmingsson, N. T. Son, O. Kordina, J. P. Bergman, E. Janzén, J. L. Lindström, S. Savage, and N. Nordell, J. Appl. Phys. **81**, 6155 (1997).
[7] G. Alfieri, E. V. Monakhov, B. G. Svensson, and M. K. Linnarsson, J. Appl. Phys. **98**, 043518 (2005).
[8] M. L. David, G. Alfieri, E. M. Monakhov, A. Hallén, C. Blanchard, B. G. Svensson, and J. F. Barbot, J. Appl. Phys. **95**, 4728 (2004).
[9] S. G. Sridhara, L. L. Clemen, R. P. Devaty, W. J. Choyke, D. J. Larkin, H. S. Kong, T. Troffer, and G. Pensl, J. Appl. Phys. **83**, 7909 (1998).
[10] G. Alfieri and T. Kimoto, J. Appl. Phys. **101**, 103716 (2007).
[11] T. Troffer, M. Schadt, T. Frank, H. Itoh, G. Pensl, J. Heindl, H. P. Strunk, and M. Maier, Physica Status Solidi A **162**, 277 (1997).
[12] S. Mitra, M. V. Rao, N. Papanicolaou, K. A. Jones, M. Derenge, O. W. Holland, R. D. Vispute, and S. R. Wilson, J. Appl. Phys. **95**, 69 (2004).
[13] J. Wong-Leung and B. G. Svensson, Appl. Phys. Lett. **92**, 142105 (2008).
[14] K. Kawahara, G. Alfieri, and T. Kimoto, J. Appl. Phys. **106**, 013719 (2009).
[15] Y. Negoro, T. Kimoto, and H. Matsunami, J. Appl. Phys. **98**, 043709 (2005).
[16] D. Åberg, A. Hallén, and B. G. Svensson, Physica B **273–274**, 672 (1999).
[17] V. Khemka, T. Chow, and R. Gutmann, J. Electron. Mater. **27**, 1128 (1998).
[18] J. F. Ziegler, M. D. Ziegler, and J. P. Biersack, Nucl. Instrum. Methods Phys. Res. B **268**, 1818 (2010).
[19] G. S. Oehrlein, Mater. Sci. Eng., B **4**, 441 (1989).
[20] J. I. Pankove, R. O. Wance, and J. E. Berkeyheiser, Appl. Phys. Lett. **45**, 1100 (1984).
[21] T. Dalibor, H. Trageser, G. Pensl, T. Kimoto, H. Matsunami, D. Nizhner, O. Shigiltchoff, and W. J. Choyke, Mater. Sci. Eng., B **61–62**, 454 (1999).
[22] K. Danno, D. Nakamura, and T. Kimoto, Appl. Phys. Lett. **90**, 202109 (2007).
[23] G. Alfieri, E. V. Monakhov, B. G. Svensson, and A. Hallén, J. Appl. Phys. **98**, 113524 (2005).
[24] T. Hiyoshi and T. Kimoto, Appl. Phys. Express **2**, 041101 (2009).

Downloaded 19 Jun 2011 to 130.54.110.71. Redistribution subject to AIP license or copyright; see http://jap.aip.org/about/rights_and_permissions